

UCLA

UCLA Previously Published Works

Title

Origin of π -Facial Stereoselectivity in Thiophene 1-Oxide Cycloadditions

Permalink

<https://escholarship.org/uc/item/8xs6440f>

Journal

The Journal of Organic Chemistry, 83(5)

ISSN

0022-3263

Authors

Levandowski, Brian J
Herath, Dinushka
Gallup, Nathan M
[et al.](#)

Publication Date

2018-03-02

DOI

10.1021/acs.joc.7b03016

Peer reviewed



Published in final edited form as:

J Org Chem. 2018 March 02; 83(5): 2611–2616. doi:10.1021/acs.joc.7b03016.

Origin of π -Facial Stereoselectivity in Thiophene 1-Oxide Cycloadditions

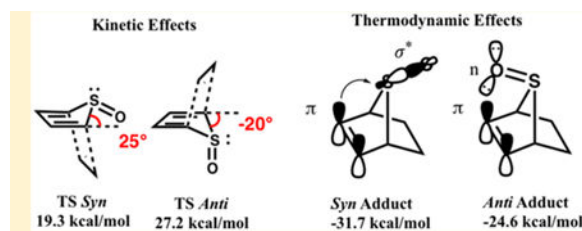
Brian J. Levandowski, Dinushka Herath, Nathan M. Gallup, and K N Houk*

Department of Chemistry and Biochemistry, University of California, Los Angeles, California 90095, United States

Abstract

We report a DFT computational study (M06–2X) of π -facial selectivity in the Diels—Alder reactions of thiophene 1-oxide. The preference for the *syn* cycloaddition arises because the ground state geometry of thiophene 1-oxide is predistorted into an envelope conformation that resembles the *syn* transition state geometry. The *syn* distortion occurs to minimize the effect of hyperconjugative antiaromaticity in the thiophene 1-oxide, arising from overlap of the σ^*_{SO} with the π -system. The *syn* selectivity follows through to the product structure that is stabilized by a π — σ^*_{SO} interaction, related to the 7-norbornenyl ion stability.

Graphical Abstract



INTRODUCTION

The high reactivities, selectivities, and yields of thiophene 1-oxide cycloadditions warrant their classification as click reactions, alongside the useful and well studied inverse electron-demand Diels—Alder reactions of tetrazines.¹ Thiophene 1-oxides react with electron-rich, electron-neutral, and electron-deficient dienophiles in the Diels—Alder reaction with exclusive *syn* π -facial stereoselectivity, as shown in Scheme 1.^{2–10} *Syn* refers to the reaction where the dienophile adds *syn* to the oxygen.

Correspondence to: K N Houk.

*Corresponding Author houk@chem.ucla.edu.

ASSOCIATED CONTENT

Supporting Information

The Supporting Information is available free of charge on the ACS Publications website at DOI: 10.1021/acs.joc.7b03016. Cartesian coordinates and energies of all optimized structures and transition structures (PDF)

Notes

The authors declare no competing financial interest.

Previously proposed explanations for the *syn* π -facial stereoselectivity in thiophene 1-oxide Diels—Alder reactions are summarized in Scheme 2. Fallis et al. reported X-ray crystal structures for the thiophene 1-oxide adducts with a series of dienophiles and attributed the *syn* π -facial stereoselectivity to the Cieplak Effect.² In the Cieplak model, stereoselectivity is controlled by hyperconjugation between an antiperiplanar donor orbital and the σ^* acceptor orbitals of the incipient bonds in the transition state.^{11,12} The lone pair on sulfur in thiophene 1-oxide is a stronger donor compared to the S=O bond of the sulfoxide moiety. The Cieplak model correctly predicts that dienophiles will attack *anti* to the sulfur lone pair and *syn* to the sulfoxide oxygen (Scheme 2a).

An extensive experimental and computational study by Nakayama showed that thiophene 1-oxide Diels—Alder reactions are inverse electron-demand reactions with electron- rich, electron-neutral, and electron-deficient dienophiles.⁸ They computed the *syn* and *anti* transition state geometries and reported that the envelope geometry of the thiophene 1-oxide ground state requires less geometrical change of the S=O bond about the plane of the diene to achieve the *syn* transition state geometry (Scheme 2b). Additionally, a destabilizing interaction in the *anti* transition state involving the nonbonding sulfur lone pair with the HOMO of the dienophile was proposed as a potential factor disfavoring the *anti* transition state (Scheme 2c).^{10c} Because of our theoretical interest in the reactivity and stereoselectivity of 5-X-cyclopentadienes¹³ and heterocyclic analogues,¹⁴ and of the distortion/interaction activation-strain¹⁵ method of analysis, we have reinvestigated this phenomenon. We have found that hyperconjugative antiaromaticity in the thiophene 1-oxide ground state and distortion energies control stereoselectivity.

COMPUTATIONAL METHODS

Computations were performed in Gaussian 09, revision D.0.1.¹⁶ with the M06–2X density functional that provides accurate energies for cycloaddition reactions.¹⁷ Geometry optimizations and single point energies reported here were computed with the 6–31+G(d) and 6–311++G(d,p) basis sets, respectively. Truhlar’s quasiharmonic correction was applied by setting all positive frequencies below 100 cm⁻¹ to a value of 100 cm⁻¹.¹⁸

RESULTS AND DISCUSSION

Figure 1 shows the activation free energies (ΔG^\ddagger) for the *syn*- and *anti-endo* Diels—Alder reactions of thiophene 1-oxide with cyclopentene (**1**), cyclopentenone (**2**), and 2,3-dihydrofuran (**3**). The *syn-endo* reactions are favored by 7–8 kcal/mol relative to the *anti-endo* transition state. The activation free energies for the *syn-exo* and *anti-exo* reactions are 4–5 and 2 kcal/mol higher in energy than the *syn-endo* and *anti-endo* reactions, respectively.

We computed the *syn* and *anti* transition structures and adducts for the Diels—Alder reaction with the simplest dienophile, ethylene (Figure 2), to study the intrinsic selectivity of thiophene 1-oxide. The Diels—Alder transition structures for both the *anti* and *syn* transition states with ethylene are synchronous with forming bond lengths of 2.29 Å. The *syn* reaction is favored kinetically and thermodynamically. The reactions are exothermic with reaction free energies of –32 and –25 kcal/mol for the *syn* and *anti* adducts, respectively. The

activation free energies are 19 and 27 kcal/mol for the *syn* and *anti* transition states, respectively.

We have analyzed the differences in the transition state energies with the distortion/interaction activation-strain model.¹⁵ This model dissects the activation energy into two energetic terms: distortion energy (E_{d}^{\ddagger}) is the energy required to geometrically deform the ground state geometries of the reacting diene and dienophile into their respective transition state geometries; interaction energy (E_{i}^{\ddagger}) is calculated as the difference between the activation energy (E^{\ddagger}) and the distortion (strain) energy ($E_{\text{d}}^{\ddagger} = E^* - \Delta E_{\text{d}}^{\ddagger}$) and represents the strength of the interactions between the distorted diene and dienophile at the transition state. The interaction energies include the effects of electrostatic interactions, closed shell repulsions (steric effects), dispersion, and charge transfer between the occupied orbitals (HOMO) of one reacting species with the unoccupied orbitals (LUMO) of the other reacting species.¹⁹

The distortion/interaction analysis was performed on the *syn* and *anti* transition states of the thiophene 1-oxide Diels—Alder reaction with ethylene. Figure 3 shows that the 8 kcal/mol preference for the *syn* transition state results from the difference in the diene distortion energies. It requires 17 kcal/mol to distort the thiophene 1-oxide into the geometry of the *anti* transition state, whereas the *syn* transition state requires only 11 kcal/mol. The interaction and dienophile distortion energies of the *syn* and *anti* transition states each exhibit a 1 kcal/mol preference for the *syn* addition.

Figure 4 shows a side view of the thiophene 1-oxide ground state and of the *syn* and *anti* transition states with ethylene. The π — σ^* hyperconjugative interaction between the diene π -bonds and the σ^*_{SO} bond destabilizes the thiophene-1-oxide by inducing the 4π antiaromatic character in the diene.²⁰ The sulfur lone pair interaction with the diene is a stabilizing 6π interaction, but the sulfur atom is tetrahedral with the lone pair mainly *s* in character and not appreciably overlapping with the diene π -system.²¹ To minimize the destabilizing effect of the hyperconjugative antiaromaticity, the S=O bond distorts away from the plane of the diene and the thiophene 1-oxide adopts an envelope geometry with CSC plane folded 8° above the plane of the diene. The same predistortion has been observed in 5-fluorocyclopentadiene to minimize the destabilizing π — σ^*_{CF} bond interaction.^{13b}

The difference in the distortion energies of the *syn* and *anti* transition states controlling the π -facial stereoselectivity is consistent with Nakayama's explanation involving the conformational change of the thiophene 1-oxide.⁸ In the *syn* and *anti* transition state structures, the CSC plane is distorted 25° and —20° relative to the plane of the diene, respectively. As a result of the 8° predistortion toward the *syn* envelope geometry, the *anti* transition state requires an additional distortion of 11° about the CSC plane compared to the *syn* transition state (see Figure 4).

The origin of the 7 kcal/mol difference between the stabilities of the *syn* and *anti* adducts has not been resolved in literature. Lemal et al. computationally investigated the differences in product stabilities through an isodesmic reaction that relates the energies of the *syn* and *anti* adducts to a saturated analogue.²² The isodesmic reaction suggests the presence of a

stabilizing interaction in the *syn* adduct, but they were unable to identify the nature of the stabilizing interaction.

Scheme 3 shows the hydrogenation enthalpies (ΔH) for the addition of H_2 across the double bond of the *syn* and *anti* adducts and a dioxide analogue for reference. This analysis points to the presence of a 3–4 kcal/mol stabilizing interaction involving the π -bond of the *syn* adduct and a 3–4 kcal/mol destabilizing interaction involving the π -bond of the *anti* adduct. Figure 5a shows a stabilizing hyperconjugative π – σ^* interaction between the alkene π -bond and the σ^* of the S–O bond in the *syn* adduct that accounts for the *syn* thermodynamic preference. The π – σ^* hyperconjugative interaction is not present in the *anti* adduct because the π -bond and the σ^*_{SO} are not antiperiplanar. The natural bonding orbitals (NBOs) of the discussed π_{CC} and σ^*_{SO} orbitals are shown in Figure 5b,c. We used second-order perturbation theory calculations provided by Natural Bond Orbital (NBO 3.1)²³ analysis to quantify the strength of the π_{CC} – σ^*_{SO} interaction. The NBO analysis calculated the strength of the π_{CC} – σ^*_{SO} interaction to be 2.9 kcal/mol in the *syn* adduct, consistent with our prediction from the hydrogenation reactions.

Evidence of π – σ^* interactions have been spectroscopically observed in norbornen-7-yl fluorides.²⁴ When the double bond is *anti* to the C–F bond in the norbornen-7-yl fluoride, the π – σ^*_{CF} interaction causes a large downfield fluoride shift.

Figure 6 shows a repulsive n – π interaction between the nonbonding oxygen lone pair of the sulfoxy moiety and the $\pi_{C=C}$ bond that is destabilizing in the *anti* adduct. The combination of the stabilizing π – σ^* interaction in the *syn* adduct and the destabilizing repulsive n – π interaction in the *anti* adduct result in the 7 kcal/mol thermodynamic preference for the *syn* adduct.

Lemal reported that thiophene 1-oxides rapidly dimerize, while thiophene 1,1-dioxides are less prone to dimerization.^{22,25} The free energy profile for the Diels–Alder reaction of thiophene 1,1-dioxide with ethylene is shown in Figure 7. The activation free energy barrier is 26 kcal/mol, similar to the barrier of the thiophene 1-oxide *anti* cycloaddition. Comparatively, the *syn* reaction of thiophene 1-oxide with ethylene has a lower barrier of only 19 kcal/mol (see Figure 2).

The frontier molecular orbital (FMO) analysis of thiophene 1-oxide and thiophene 1,1-dioxide with ethylene is shown in Figure 8. Both dienes are inverse electron-demand where the principal interaction is the HOMO of ethylene and the LUMO of the diene. FMO theory predicts that thiophene 1-oxide with a larger FMO gap should be less reactive than thiophene 1,1-dioxide in the inverse electron-demand Diels–Alder reaction with ethylene.

To understand why thiophene 1-oxide is more reactive than thiophene-1,1-dioxide in the Diels–Alder reaction with ethylene, we analyzed the reaction pathways from a reaction complex with average carbon–carbon bond forming lengths of 2.8 Å to the transition state geometries using the distortion/ interaction-activation strain model.¹⁵ Figure 9 shows that the differences in the Diels–Alder reactivities of thiophene 1-oxides and thiophene 1,1-dioxides result from differences in the distortion energies.

As shown in Figure 10, the ground state geometry of the thiophene 1,1-dioxide is planar and requires a folding of 22° to achieve the envelope geometry of the transition state. Thiophene 1-oxides are more reactive than thiophene 1,1-dioxides because the ground state geometries of thiophene 1-oxides are predistorted toward the envelope geometries of the *syn* transition states. This is consistent with our previous prediction that 5-fluorocyclopentadiene, which adopts an envelope geometry in the ground state to minimize the effect of the $\pi-\sigma^*_{CF}$ antiaromatic hyperconjugative interaction, is more reactive than the planar 5,5-difluorocyclopentadiene in Diels—Alder reactions.^{13b}

CONCLUSION

Analysis of the *syn* and *anti* Diels—Alder reactions with the distortion/interaction-activation strain model reveals that the kinetic preference for the *syn* adduct parallels the differences in the thiophene 1-oxide distortion energies. To reduce the destabilizing effect of hyperconjugative aromaticity, the thiophene 1-oxide is predistorted into an envelope geometry that more closely resembles the envelope geometry of the *syn* transition state. This effect results in the observed *syn* stereoselectivity and high reactivity of thiophene 1-oxide Diels—Alder reactions. The thermodynamic preference for the *syn* adduct is the result of a stabilizing $\pi-\sigma^*_{SO}$ interaction in the *syn* adduct and a destabilizing $n-\pi$ interaction in the *anti* adduct.

Supplementary Material

Refer to Web version on PubMed Central for supplementary material.

ACKNOWLEDGMENTS

We are grateful to the National Science Foundation (CHE- 1361104) and the National Institute of Health (R01 GM109078) for financial support of this research. Computer time was provided by the UCLA Institute for Digital Research and Education (IDRE). We also thank Dr. Trevor Hamlin for helpful discussions. We thank Professor Claude Y. Legault for CYLview,²⁶ which was used to generate images of the optimized structures.

REFERENCES

- (1). (a) Jewett JC; Bertozzi CR Chem. Soc. Rev. 2010, 39, 1272. [PubMed: 20349533] (b)Liu F; Liang Y; Houk KN Acc. Chem. Res. 2017, 50, 2297. [PubMed: 28876890]
- (2). Naperstkw AM; Macaulay JB; Newlands MJ; Fallis AG Tetrahedron Lett. 1989, 30, 5077.
- (3). Treiber A; Dansette PM; Amri HE; Girault JP; Ginderow D; Mornon JP; Mansuy DJ J. Am. Chem. Soc. 1997, 119, 1565.
- (4). Li Y; Thiemann T; Sawada T; Mataka S; Tashiro MJ Org. Chem. 1997, 62, 7926.
- (5). Furukawa N; Zhang S-Z; Horn E; Takahashi O; Sato S Heterocycles 1998, 47, 793.
- (6). Li YQ; Thiemann T; Mimura K; Sawada T; Mataka S; Tashiro M Eur. J. Org. Chem. 1998, 1998, 1841.
- (7). Otani T; Takayama J; Sugihara Y; Ishii A; Nakayama JJ Am. Chem. Soc. 2003, 125, 8255.
- (8). Takayama J; Sugihara Y; Takayanagi T; Nakayama J Tetrahedron Lett. 2005, 46, 4165.
- (9). Thiemann T; Iniesta J; Walton DJ Phosphorus. Phosphorus, Sulfur Silicon Relat. Elem. 2016, 191, 876.
- (10). For reviews, see: (a) Nakayama J; Sugihara Y Sulfur Rep. 1997, 19, 349.(b)Nakayama J Sulfur Rep. 2000, 22, 123.(c)Ishida M;Inagaki S Orbitals in Chemistry; Inagaki S, Ed.; Springer-Verlag: Berlin, 2009; Vol. 289, p 183.

- (11). (a) Cieplak AS *J. Am. Chem. Soc.* 1981, 103, 4540.(b)Cieplak AS; Tait BD; Johnson CR *J. Am. Chem. Soc.* 1989, 111, 8447.
- (12). (a) Macaulay JB; Fallis AG *J. Am. Chem. Soc.* 1990, 112, 1136.(b)Coxon JM; McDonald DQ *Tetrahedron Lett.* 1992, 33, 651.
- (13). (a) Levandowski BJ; Hamlin TA; Bickelhaupt FM; Houk KN *J. Org. Chem.* 2017, 82, 866.
(b)Levandowski BJ; Zou L; Houk KN *J. Comput. Chem.* 2016, 37, 117. [PubMed: 26444427]
(c)Levandowski BJ; Houk KN *J. Org. Chem.* 2015, 80, 3530. [PubMed: 25741891]
- (14). Fell JS; Martin BM; Houk KN *J. Org. Chem.* 2017, 82, 1912–1919. [PubMed: 28150495]
- (15). Bickelhaupt FM; Houk KN *Angew. Chem. Int. Ed.* 2017, 56, 2.
- (16). Frisch MJ; Trucks GW; Schlegel HB; Scuseria GE; Robb MA; Cheeseman JR; Scalmani G; Barone V; Mennucci B; Petersson GA; Nakatsuji H; Caricato M; Li X; Hratchian HP; Izmaylov AF; Bloino J; Zheng G; Sonnenberg JL; Hada M; Ehara M; Toyota K; Fukuda R; Hasegawa J; Ishida M; Nakajima T; Honda Y; Kitao O; Nakai H; Vreven T; Montgomery JA, Jr.; Peralta JE; Ogliaro F; Bearpark M; Heyd JJ; Brothers E; Kudin KN; Staroverov VN; Kobayashi R; Normand J; Raghavachari K; Rendell A; Burant JC; Iyengar SS; Tomasi J; Cossi M; Rega N; Millam MJ; Klene M; Knox JE; Cross JB; Bakken V; Adamo C; Jaramillo J; Gomperts R; Stratmann RE; Yazyev O; Austin AJ; Cammi R; Pomelli C; Ochterski JW; Martin RL; Morokuma K; Zakrzewski VG; Voth GA; Salvador P; Dannenberg JJ; Dapprich S; Daniels AD; Farkas O; Foresman JB; Ortiz JV; Cioslowski J; Fox DJ *Gaussian 09, revision D.01*; Gaussian, Inc.: Wallingford, CT, 2009.
- (17). Zhao Y; Truhlar DG *Theor. Chem. Acc.* 2008, 120, 215.
- (18). Zhao Y; Truhlar DG *Phys. Chem. Chem. Phys.* 2008, 10, 2813. [PubMed: 18464998]
- (19). Levandowski BJ; Houk KN *J. Am. Chem. Soc.* 2016, 138, 16731. [PubMed: 27977194]
- (20). (a) Nyulászai L; Schleyer P. v. R. *J. Am. Chem. Soc.* 1999, 121, 6872.(b)Nyulászai L; Karpati T; Schleyer P. v. R. *Eur. J. Org. Chem.* 2003, 10, 1923.
- (21). (a) Mock WL *J. Am. Chem. Soc.* 1970, 92, 7610.(b)Pouzet P; Erdelmeier I; Ginderow D; Mornon J-P; Dansette P; Mansuy DJ *Chem. Soc., Chem. Commun.* 1995, 0, 473.(c)Pouzet P; Erdelmeier I; Ginderow D; Mornon J-P; Dansette P; Mansuy DJ *Heterocycl. Chem.* 1997, 34, 1567.(d)Nakayama J; Yu T; Sugihara Y; Ishii A *Chem. Lett.* 1997, 26, 499.
- (22). Lemal DM; Akashi M; Lou Y; Kumar VJ *Org. Chem.* 2013, 78, 12330.
- (23). Glendening ED; Reed AE; Carpenter JE; Weinhold F *NBO, version 3.1*.
- (24). Adcock W; Angus DI; Lowe DA *Magn. Reson. Chem.* 1996, 34, 675.
- (25). Lemal DM *J. Org. Chem.* 2016, 81, 4931. [PubMed: 27246658]
- (26). Legault CY *CYLview, 1.0b*; Université de Sherbrooke: Sherbrooke, QC, Canada, 2009; <http://www.cylview.org>.

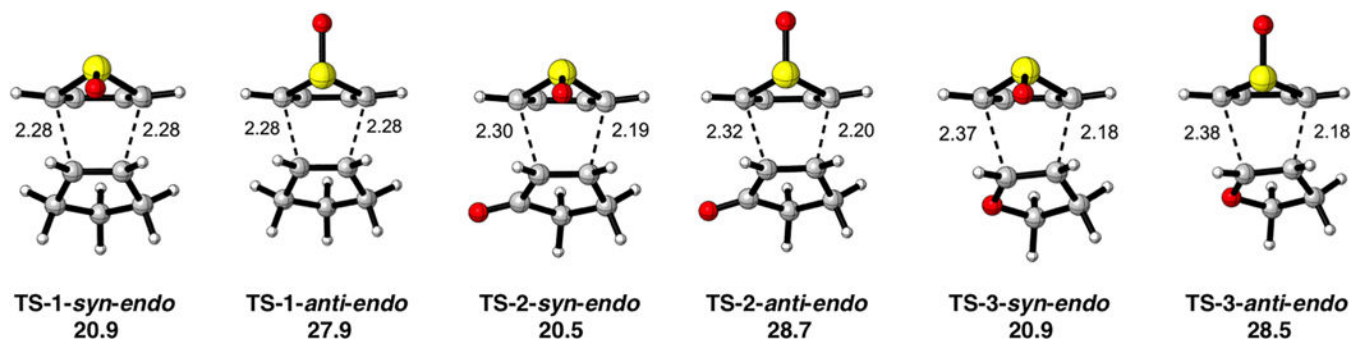


Figure 1. Activation free energies in kcal/mol for the *syn*- and *anti-endo* Diels–Alder reactions of thiophene 1-oxide with cyclopentene (**TS-1**), cyclopentenone (**TS-2**), and 2,3-dihydrofuran (**TS-3**).

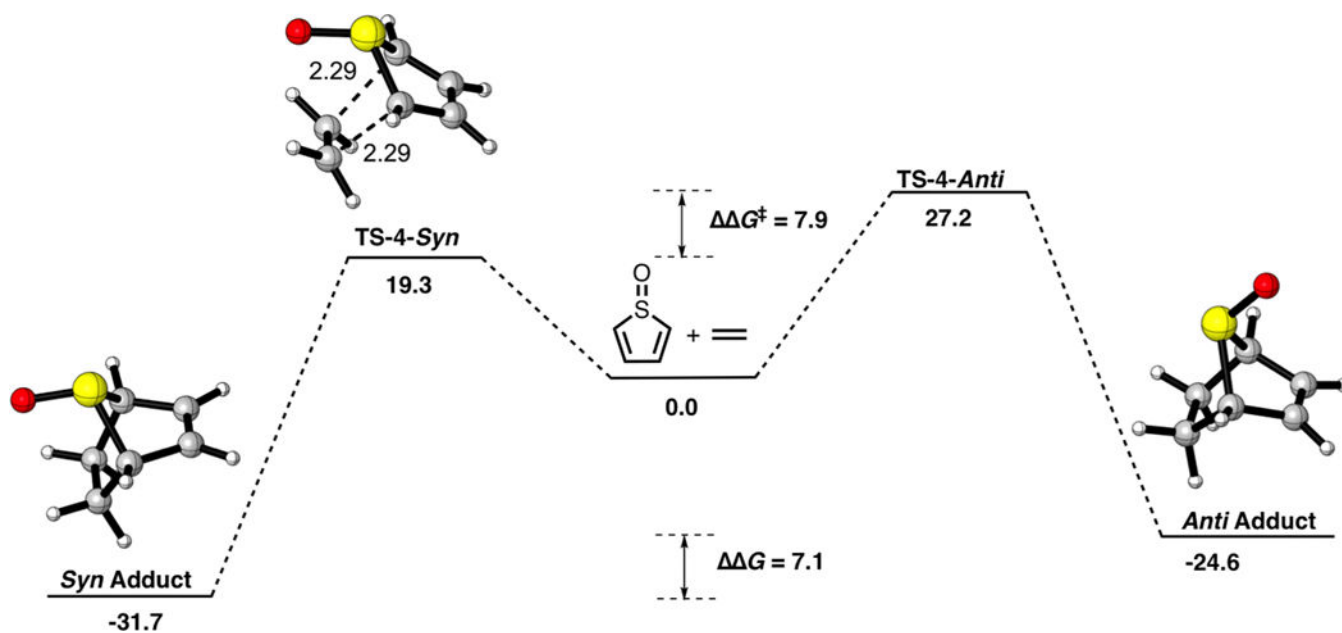


Figure 2. Computed reaction profile for the *syn* and *anti* Diels–Alder reactions of thiophene 1-oxide with ethylene. Bond lengths are reported in angstroms (Å), and free energies are reported in kcal/mol.

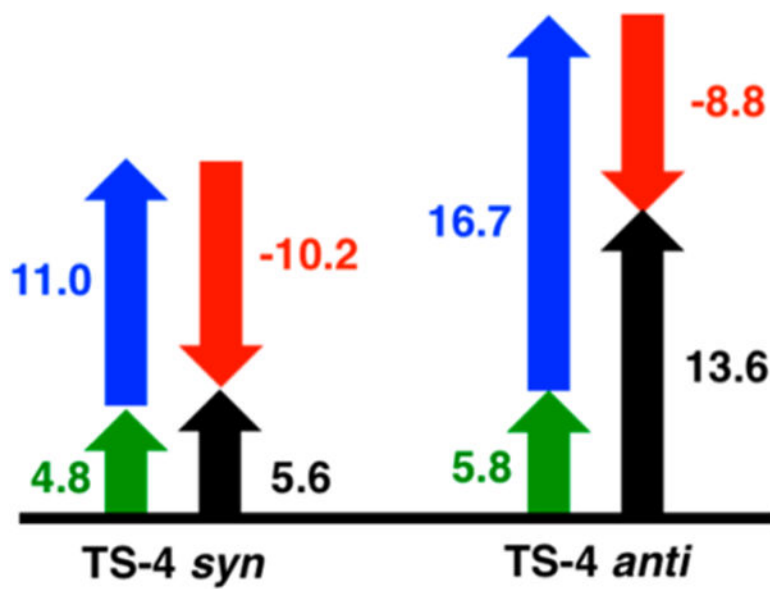


Figure 3. Distortion/interaction analysis for the *syn* and *anti* transition structures for the Diels—Alder reaction of thiophene 1-oxide with ethylene (black, activation energy; green, distortion energy of the dienophile; blue, distortion energy of the diene; red, interaction energy; in kcal/mol).

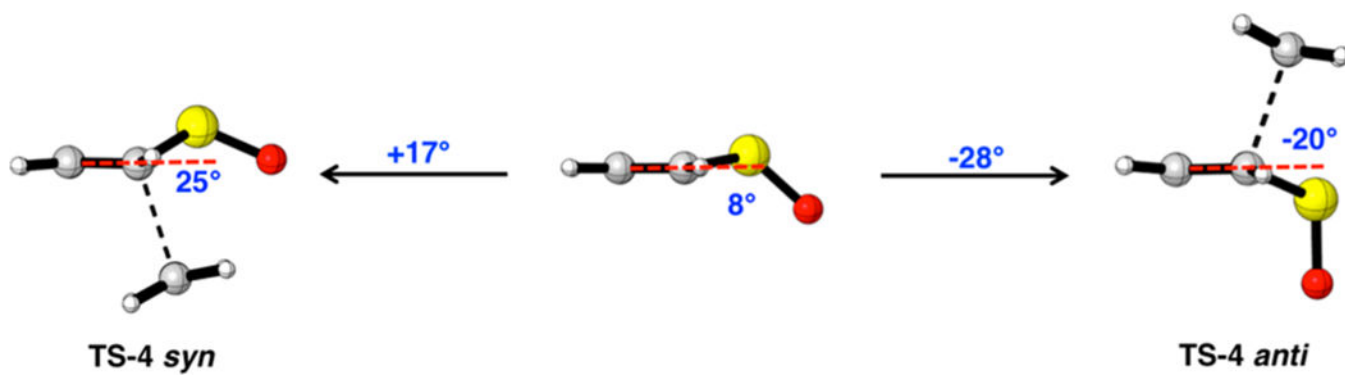


Figure 4. Side view of the thiophene 1-oxide ground state and the *syn* and *anti* transition states with ethylene. The out-of-plane bending of the sulfur atom from the plane of the diene is shown in degrees. The plane of the diene is represented by the red dashed lines.

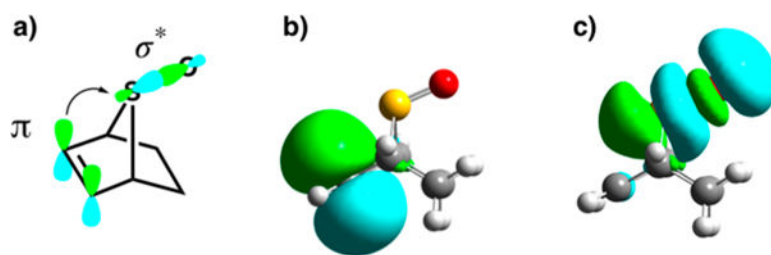


Figure 5.
(a) Stabilizing $\pi-\sigma^*_{SO}$ interaction in the *syn* adduct. (b) Visualized π_{CC} NBO. (c) Visualized σ^*_{SO} NBO.

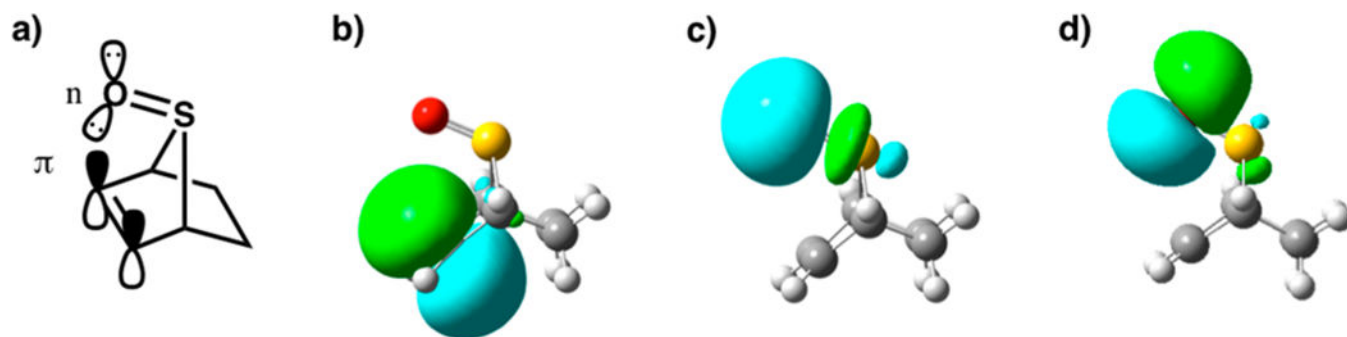


Figure 6.

(a) Repulsive $n-\pi$ interaction that destabilizes the *anti* adduct. (b) Visualized π_{cc} NBO. (c) *s*-Type lone pair of sulfoxide oxygen. (d) *p*-Type lone pair of sulfoxide oxygen.

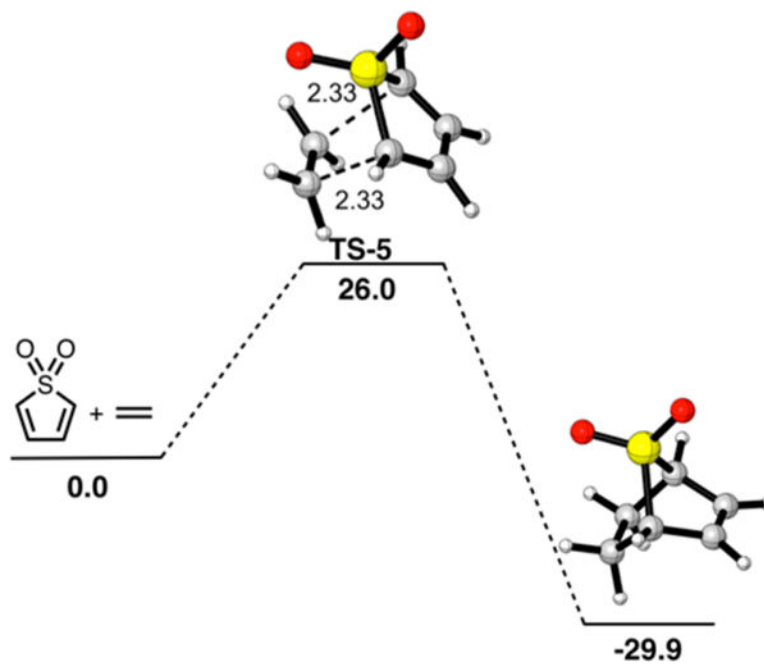


Figure 7. Free energy profile for the Diels—Alder reaction of thiophene 1,1-dioxide with ethylene. Forming bond lengths are reported in Å, and end energies are reported in kcal/mol.

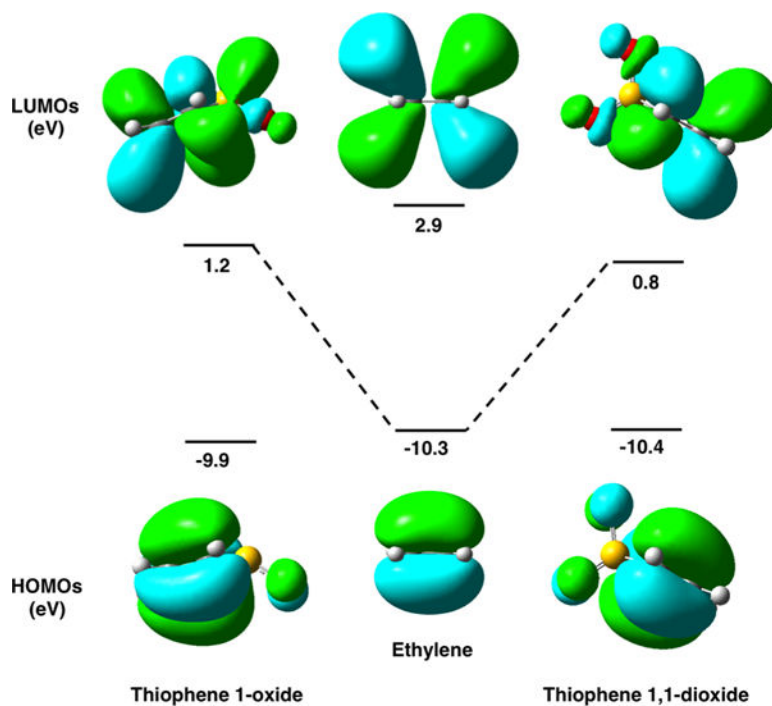


Figure 8. Frontier molecular orbitals of thiophene 1-oxide, thiophene 1,1-dioxide, and ethylene with energies reported in electron volts (eV). Frontier molecular orbital energies computed at the HF/6-311+ +G(d,p)//M06-2X/6-31+G(d) level of theory.

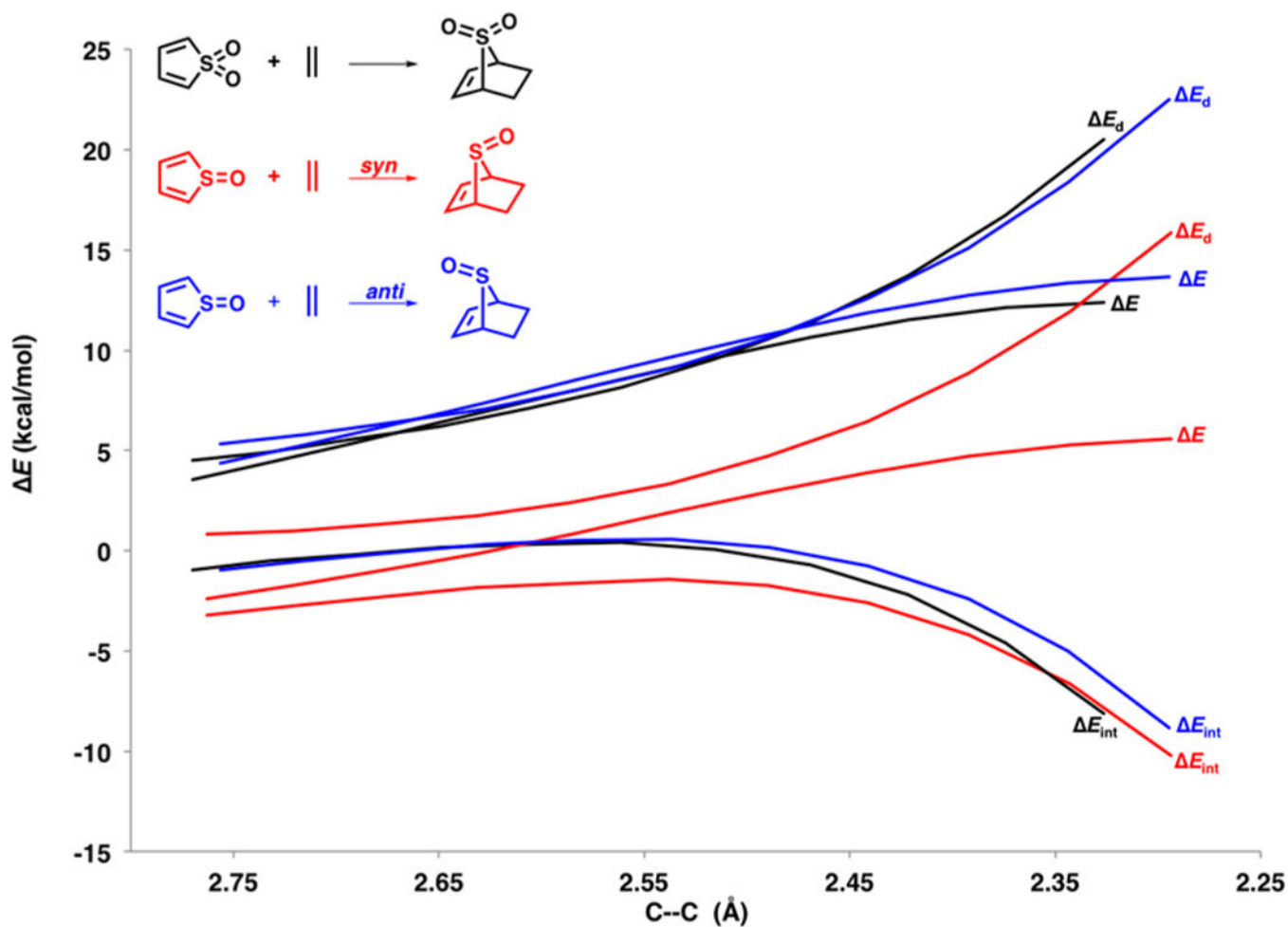


Figure 9. Distortion/Interaction-activation strain analysis for the *syn* (red) and *anti* (blue) Diels–Alder reactions of thiophene 1-oxide with ethylene and the Diels–Alder reaction of thiophene 1,1-dioxide with ethylene (black). Electronic activation energies (E), distortion energies (E_d), and interaction energies (E_i).

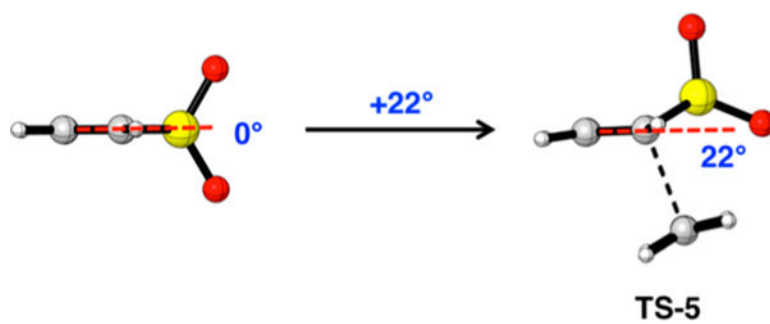
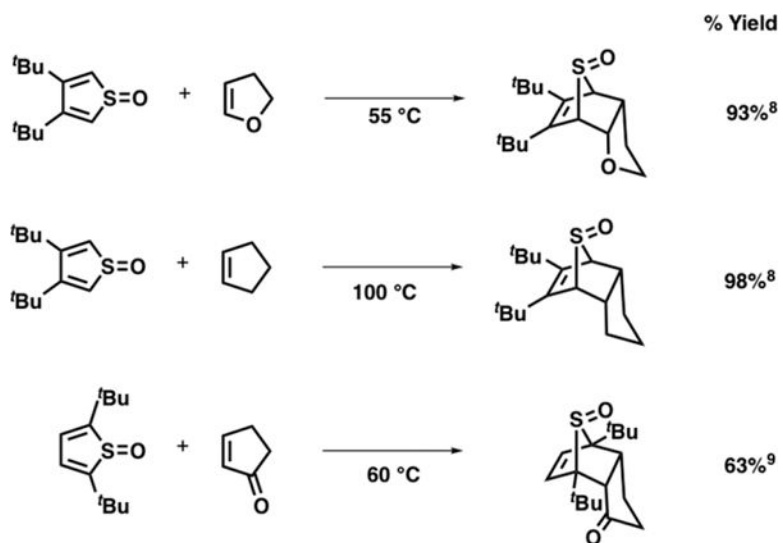
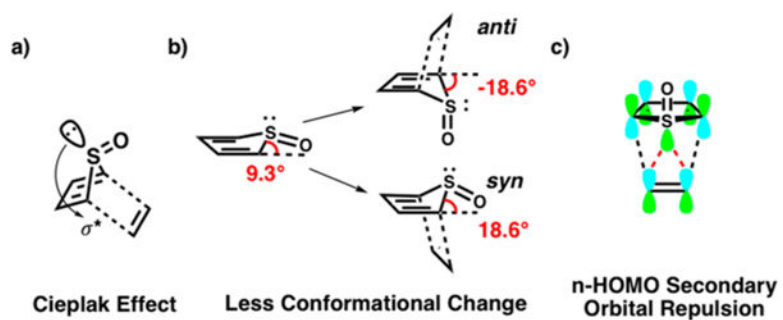


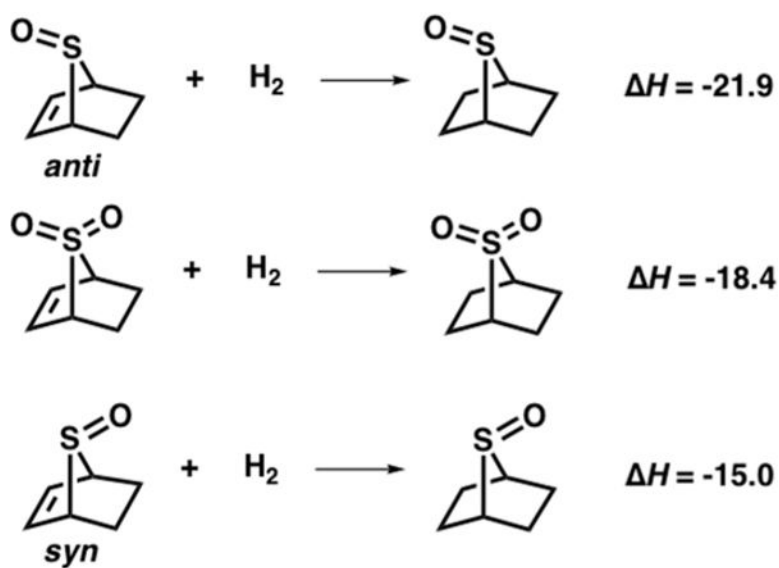
Figure 10. Planar geometry of the thiophene 1,1-dioxide and envelope geometry of the thiophene 1,1-oxide transition state with ethylene. The plane of the diene is represented with a red line.



Scheme 1.
syn Stereoselectivity in Diels—Alder Reactions of Thiophene 1-Oxides with Three Dienophiles

**Scheme 2.**

Previous Explanations for the syn π -Facial Stereoselectivity of Thiophene 1-Oxide Diels—Alder Reactions



Scheme 3.
Enthalpies of Hydrogenation (ΔH) in kcal/mol for the *syn* and *anti* Diels—Alder Adducts and an Oxidized Analogue